PHYSOR 2004 -The Physics of Fuel Cycles and Advanced Nuclear Systems: Global Developments
Chicago, Illinois, April 25-29, 2004, on CD-ROM, American Nuclear Society, Lagrange Park, IL. (2004)

Implementation of a Full P_1 Method in the Diffusion Code DONJON/NDF

Jean Koclas[1] and Benoit Forget[2]
[1]*Institut de génie nucléaire, École Polytechnique de Montréal,*
CP 6079 Montreal, Quebec, Canada H3C 3A7
[2]*Nuclear and Radiological Engineering, Georgia Institute of Technology,*
Atlanta, GA 30332, USA

Rigorous diffusion theory is obtained by the spherical harmonics expansion of the angular variable in the Boltzman transport equation, truncated to first order terms. This is known as the P_1 approximation. Diffusion coefficients do not arise naturally from this approach, and are not necessary at all. The relationships between fluxes and currents appear through terms involving anisotropic scattering cross-sections. This method gives a more accurate representation of the Boltzman equation than standard diffusion theory. The P_1 method enables slightly more accurate calculations at heterogeneous interfaces. The method was programmed as a part of the DONJON/NDF package for both the static and dynamic cases in multi-group mesh centered finite differences. The coupling coefficients that are diagonal matrices with diffusion coefficients become full matrices because of the anisotropic scattering cross-sections. Several comparisons between standard diffusion theory and the P_1 approximation are presented, including some simple transients of a typical CANDU-6 reactor model.

KEYWORDS: ***P1 method, spherical harmonics, reactor statics, reactor kinetics***

1. Introduction

Diffusion theory is considered sufficient for full core design calculations for the present reactor technology. Successful simulations and operation of multiple reactors has validated the general aspects of diffusion theory. There still exist certain spatial regions for which the predictions of standard diffusion theory differ significantly from measurements. This is true notably in the areas which offer important heterogeneities, in which a large change in the nuclear properties is noticed. Standard diffusion theory is unable to deal with these regions correctly [5], [6]. Obvious examples are the core-reflector interface, or the proximity of control devices. This is in part due to the approximation imbedded in Fick's law which is used to relate the flux gradient to the current. In effect, Fick's law enforces a hypothesis of linear anisotropy within a given energy group.

This study sets aside Fick's law by taking the complete set of equations obtained from the spherical harmonics method (P_1). This method does not rely on diffusion coefficients in order to obtain a complete P_1 solution of the Boltzman transport equation.

The complete P_1 method was programmed as a part of the DONJON/NDF [8] package. The new modules use the multi-group mesh centered finite difference method and implement both static and dynamic calculations. Most of the options that are

available in the original module of NDF are also available in these new modules. The main difference in the method is the presence of the Σ_{s1} anisotropic cross-sections and the absence of diffusion coefficients. For homogenous regions, the resulting solution is essentially identical to standard diffusion theory. However in the presence of abrupt changes in nuclear properties at the interface of a moderating medium and fuel, we observe some noticeable variations. The complete P_1 method demands slightly longer calculation time than the standard diffusion counterpart, due to the presence of additional anisotropic terms.

This study analyses the effect of P_1 method on a reference CANDU-6 reactor and compares the results with standard diffusion calculations for a two energy group model. The complete P_1 method can be seen as a validating tool supporting the use of flux mapping and other corrective methods used in core follow-up. The comparisons will consist mostly of static calculations with and without devices. The dynamic calculations will show the effect of the movement of the central adjuster rod on reactor power.

2. Complete P_1 Method [7]

The development of the complete P_1 method starts from the Boltzman transport equation in integral-differential form. We use the notation of reference [1]:

$$\frac{1}{v}\frac{\partial}{\partial t}\phi(\vec{r},\vec{\Omega},E,t) = -\vec{\Omega}\cdot\vec{\nabla}\Psi(\vec{r},\vec{\Omega},E,t) - \Sigma_t(\vec{r},E,t)\Psi(\vec{r},\vec{\Omega},E,t) + \int_0^\infty dE'\int_{\Omega'} d\Omega\Sigma_s(\vec{r},\vec{\Omega}'\to\vec{\Omega},E'\to E,t)\Psi(\vec{r},\vec{\Omega}',E',t)$$
$$+\frac{(1-\beta)\chi^p(E)}{K_{eff}}\int_0^\infty dE'\nu\Sigma_f(\vec{r},E',t)\Psi(\vec{r},\vec{\Omega},E',t) + \sum_{e=1}^{D}\chi_e^d(E)\lambda_e C_e(\vec{r},t) \qquad (1)$$

A spherical harmonics expansion is then performed in order to obtain the complete set of P_1 equations.

$$\frac{1}{v}\frac{\partial}{\partial t}\phi(\vec{r},E,t) = -\nabla\cdot\vec{J}(\vec{r},E,t) - \Sigma_t(\vec{r},E,t)\phi(\vec{r},E)$$
$$+\chi^p(E)(1-\beta)\frac{1}{K_{eff}}\int_0^\infty \nu\Sigma_f(\vec{r},E',t)\phi(\vec{r},E',t)dE' \qquad \textbf{(2)}$$
$$+\int_0^\infty \Sigma_{s0}(\vec{r},E'\to E,t)\phi(\vec{r},E',t)dE' + \sum_{e=1}^{D}\chi_e^d(E)\lambda_e C_e(\vec{r},t)$$

and

$$\frac{1}{v}\frac{\partial}{\partial t}\vec{J}(\vec{r},E,t) + \frac{1}{3}\vec{\nabla}\phi(\vec{r},E,t) + \Sigma_t(\vec{r},E,t)\vec{J}(\vec{r},E,t)$$
$$= \int_0^\infty \Sigma_{s1}(\vec{r},E'\to E,t)\vec{J}(\vec{r},E',t)dE' \qquad (3)$$

Let us now consider the temporal derivative of the current term in equation 3. This term may be neglected by considering that the current variation is negligible compared to the probability of interaction [2],[3],[4]. Only an extremely rapid current variation would

contradict this hypothesis. Without this simplification, the current equation is the telegraph equation whose solution is a wave equation plus a diffusion equation. We then neglect the wave propagation following a perturbation. The effect should be very small considering the speed at which the neutrons travel compared to the spatial size of the reactor. Equation (3) then becomes

$$\frac{1}{3}\vec{\nabla}\phi(\vec{r},E,t)+\Sigma_t(\vec{r},E,t)\vec{J}(\vec{r},E,t)=\int_0^{\infty}\Sigma_{s1}(\vec{r},E'\to E,t)\vec{J}(\vec{r},E',t)dE' \tag{4}$$

Using the mesh centered difference method in 3D Cartesian coordinate system, after having applied multigroup theory for the energy variable, we are able to reduce the equation system in its final form after substituting Equation (4) into Equation (2):

$$\begin{aligned}
[v]_{ijk}^{-1}\frac{\partial}{\partial t}\left[\bar{\phi}\right]_{ijk}V_{ijk} &= h_y^j h_z^k\left[\frac{h_x^{i+1}}{2}\left[N_{12}\right]_{i+1jk}+\frac{h_x^i}{2}\left[N_{12}\right]_{ijk}\right]^{-1}\left[\bar{\phi}\right]_{i+1jk}\\
&+h_y^j h_z^k\left[\frac{h_x^i}{2}\left[N_{12}\right]_{ijk}+\frac{h_x^{i-1}}{2}\left[N_{12}\right]_{i-1jk}\right]^{-1}\left[\bar{\phi}\right]_{i-1jk}\\
&+h_x^i h_z^k\left[\frac{h_y^{j+1}}{2}\left[N_{12}\right]_{ij+1k}+\frac{h_y^j}{2}\left[N_{12}\right]_{ijk}\right]^{-1}\left[\bar{\phi}\right]_{ij+1k}\\
&+h_x^i h_z^k\left[\frac{h_y^j}{2}\left[N_{12}\right]_{ijk}+\frac{h_y^{j-1}}{2}\left[N_{12}\right]_{ij-1k}\right]^{-1}\left[\bar{\phi}\right]_{ij-1k}\\
&+h_x^i h_y^j\left[\frac{h_z^{k+1}}{2}\left[N_{12}\right]_{ijk+1}+\frac{h_z^k}{2}\left[N_{12}\right]_{ijk}\right]^{-1}\left[\bar{\phi}\right]_{ijk+1}\\
&+h_x^i h_y^j\left[\frac{h_z^k}{2}\left[N_{12}\right]_{ijk}+\frac{h_z^{k-1}}{2}\left[N_{12}\right]_{ijk-1}\right]^{-1}\left[\bar{\phi}\right]_{ijk-1}
\end{aligned}$$

$$\left\{\begin{array}{l}
-h_y^j h_z^k\left[\frac{h_x^{i+1}}{2}\left[N_{12}\right]_{i+1jk}+\frac{h_x^i}{2}\left[N_{12}\right]_{ijk}\right]^{-1}\\
-h_y^j h_z^k\left[\frac{h_x^i}{2}\left[N_{12}\right]_{ijk}+\frac{h_x^{i-1}}{2}\left[N_{12}\right]_{i-1jk}\right]^{-1}\\
-h_x^i h_z^k\left[\frac{h_y^{j+1}}{2}\left[N_{12}\right]_{ij+1k}+\frac{h_y^j}{2}\left[N_{12}\right]_{ijk}\right]^{-1}\\
-h_x^i h_z^k\left[\frac{h_y^j}{2}\left[N_{12}\right]_{ij-1k}+\frac{h_y^{j-1}}{2}\left[N_{12}\right]_{ij-1k}\right]^{-1}\\
-h_x^i h_y^j\left[\frac{h_z^{k+1}}{2}\left[N_{12}\right]_{ijk+1}+\frac{h_z^k}{2}\left[N_{12}\right]_{ijk}\right]^{-1}\\
-h_x^i h_y^j\left[\frac{h_z^k}{2}\left[N_{12}\right]_{ijk}+\frac{h_z^{k-1}}{2}\left[N_{12}\right]_{ijk-1}\right]^{-1}
\end{array}\right\}\left[\bar{\phi}\right]_{ijk}\quad-\left[\Sigma\right]_{ijk}\left[\bar{\phi}\right]_{ijk}V_{ijk}+(1-\beta)\left[\chi^p\right]\left[\nu\Sigma_f\right]_{ijk}^{T}\left[\bar{\phi}\right]_{ijk}V_{ijk}+\sum_{e=1}^{D}\left[\chi_e^d\right]\lambda_e\bar{C}_eV_{ijk} \tag{5}$$

where $[N_{12}]$ is given by

$$[N_{12}]=\begin{bmatrix} 3(\Sigma_{t1}-\Sigma_{s1,1\leftarrow 1}) & -3\Sigma_{s1,1\leftarrow 2} & \dots & -3\Sigma_{s1,1\leftarrow G} \\ -3\Sigma_{s1,2\leftarrow 1} & 3(\Sigma_{t2}-\Sigma_{s1,2\leftarrow 2}) & \dots & -3\Sigma_{s1,2\leftarrow G} \\ \dots & \dots & \dots & \dots \\ -3\Sigma_{s1,G\leftarrow 1} & -3\Sigma_{s1,G\leftarrow 2} & \dots & 3(\Sigma_{tG}-\Sigma_{s1,G\leftarrow G}) \end{bmatrix}$$

and V_{ijk} is the volume element equal to $h_x^i h_y^j h_z^k$, where h is the interval width in the corresponding direction. The term $\left[\bar{\phi}\right]_{ijk}$ is the node average flux and $[v]_{ijk}$ is a diagonal matrix of the neutron velocity. All other terms follow standard notation.

Note that the $[N_{12}]$ matrix differs from standard diffusion $[N_{12}]$ matrix which would be diagonal and of the form:

$$[N_{12}]=\begin{bmatrix} D_1^{-1} & 0 & \dots & 0 \\ 0 & D_2^{-1} & \dots & 0 \\ \dots & \dots & \dots & \dots \\ 0 & 0 & \dots & D_G^{-1} \end{bmatrix}$$

3. Code Description

As with every diffusion calculation, there is an interaction between a transport code and a diffusion code. The transport code used in these calculations is DRAGON [9], which is used to provide cross-section data to DONJON/NDF. No modifications were needed in DRAGON for obtaining the anisotropic scattering cross-sections. The implementation of complete P_1 method is performed in the NDF package of the DONJON code. The modifications brought to the original DONJON code are minimal. The CRE: module which reads the DRAGON cross-section data and converts it to the DONJON formalism was modified to extract the anisotropic cross-sections.

3.1 DONJON/NDF

The NDF package consists of methods utilizing nodal differences and discontinuity factors to solve the diffusion equation. The complete P_1 method was strongly based on the original modules of NDF solving the diffusion equation. The main differences appear in the matrix assembly. In the complete P_1 the $[N_{12}]$ matrix is not diagonal and includes both down-scattering and up-scattering. This full matrix forces modifications to the diffusion code, especially in the coupling coefficients. The (spatial) iteration modules also had to be modified to take into account the full matrix form of the coupling coefficients. All the iterative methods of solution that were available in the original diffusion calculation through NDF are available with the complete P_1 method for both the static and dynamic cases.

3.2 DRAGON

The complete P_1 method requires homogenized Σ_{s1} cross-sections which are calculated in the cell code. These cross-sections and all other nuclear properties used in the calculations are homogenized over the entire cell. In developing the P_1 equations, it

should be noticed that the anisotropic cross-sections should be homogenized over the current instead of the flux [1]. However this more rigorous homogenization technique was not available in DRAGON when the cell properties were calculated. The flux homogenization was used for all results reported in this paper.

The homogenization over a 2-D symmetric cell will give a single anisotropic cross-section value for all directions. This will again give linear anisotropy similar to that of the diffusion coefficients. However, the differences lie in the value of the diagonal terms and in the energy dependence terms that are present in the complete P_1 method. In the two energy group model the up-scattering cross-section is practically negligible but becomes more important with a higher number of energy groups. In heterogeneous regions composed of a moderating medium, the significance of the down-scattering term will be demonstrated. As for the diffusion coefficients, an important comparison can already be made as we can see in the next table.

TABLE 1. Comparison between nuclear properties on the diagonal.

	Group	**$1/3\Sigma_{tr}$**	**$1/3(\Sigma_t-\Sigma_{s1})$**	**% Abs. Diff.**
Fresh Fuel	*Fast*	1.272	1.290	1.4 %
	Thermal	0.920	0.921	0.1 %
Equilibrium Fuel	*Fast*	1.272	1.293	1.7 %
	Thermal	0.918	0.918	0.0 %
Reflector	*Fast*	1.277	1.277	0.0 %
	Thermal	0.887	0.888	0.1 %

These results show a difference in the fast group of the fueled cells. The effects of this variation will be explained throughout the result analysis.

4. Results

All the results, unless otherwise noted, show the difference between the flux calculated from the complete P_1 method and the original diffusion method using Fick's law. This means that a positive value indicates that the complete P_1 predicts a higher flux and vice-versa. The calculations are based on a typical CANDU-6 reactor model in two energy groups, with fourteen liquid zone controllers and twenty one adjuster rods.

4.1 Static Calculations

The static calculations were first performed for a reactor without any control devices in order to emphasize the effect of the complete P_1 method on the core-reflector interface. Some calculations were also performed with control devices. In this case, the adjusters were in nominal position (fully inserted) and the liquid control zone levels were filled halfway.

4.1.1 Without any devices

Figures 1 and 2 indicate that the flux predicted by the new method is higher in the reflector than the one predicted by the standard method. The variation is of the order of about +3% in the periphery and -1 % in the center for the thermal group. The fast group presents variations of +1.5% in the periphery and -1% in the center.

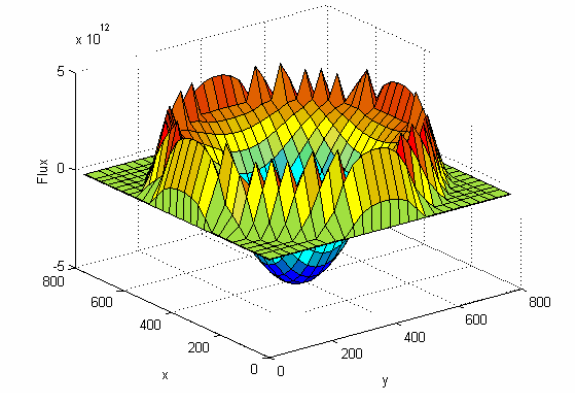

Figure 1: Difference between methods without any devices plane 6 xy (Thermal group)

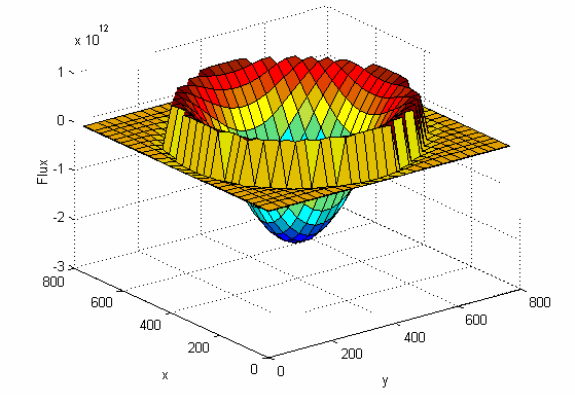

Figure 2: Difference between methods without any devices plane 6 xy (Fast group)

This distribution can easily be explained by the data shown in Table 1. Since the fast diagonal coefficient is higher in the new method and that the neutron current coming from the fuel is higher than the current from the reflector, we will in fact see a flux peak in the reflector when comparing both methods. The complete P_1 method predicts a higher fast flux scattering term than the original method, which is obviously directed towards the reflector, but both methods have similar scattering values in the reflector. This will cause a slight accumulation of neutrons in the complete P_1 method compared to the original method. Such a variation is also noticeable in the thermal group. The thermal neutron population is coupled to the fast neutron population; hence a variation in the fast flux will have repercussions in the thermal flux since the vast majority of neutrons are born fast.

Another possible reason for the higher flux in the reflector is the presence of the anisotropic down-scattering cross-section. As we will later show, this variation is negligible compared to the importance of the variation of the coupling coefficient in the fast energy group.

4.1.2 With devices

At first glance, we notice similarities between Figures 3-4 and Figures 1-2. Once again, there is a variation in the core-reflector interface which seems to dominate over all others. Closer scrutiny shows two tilts.

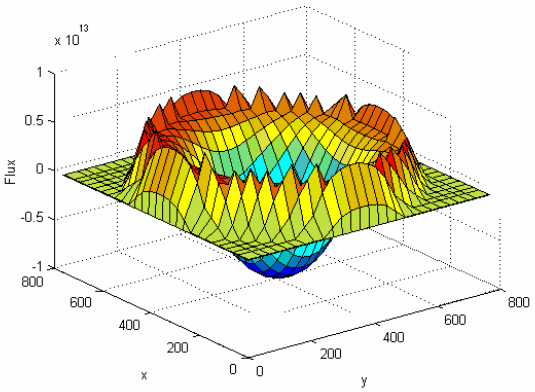

Figure 3: Difference between methods with devices plane 6 xy (Thermal group)

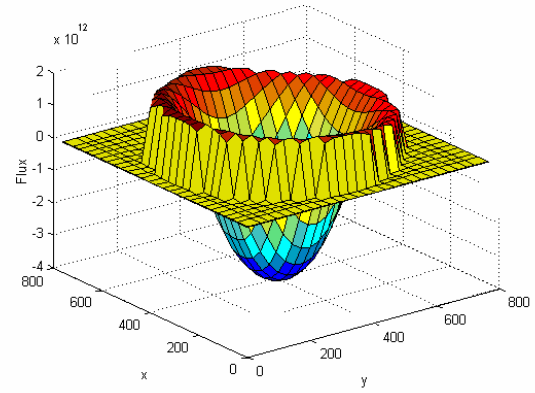

Figure 4: Difference between methods without devices plane 6 xy (Fast group)

The CANDU-6 reactor was designed with vertical liquid controllers. The bottom of these controllers is filled with light water acting as a neutron absorber and the top is filled with a gas such as helium. These devices will of course cause a slight top to bottom tilt. The filled portion will absorb neutrons while the top portion will not. The flux at the top will be higher than the one in the bottom. Figure 5 will show more clearly the effect of these devices on the flux. We have chosen a different plane than the one previously shown in order to emphasize the variations caused by the liquid zone controllers.

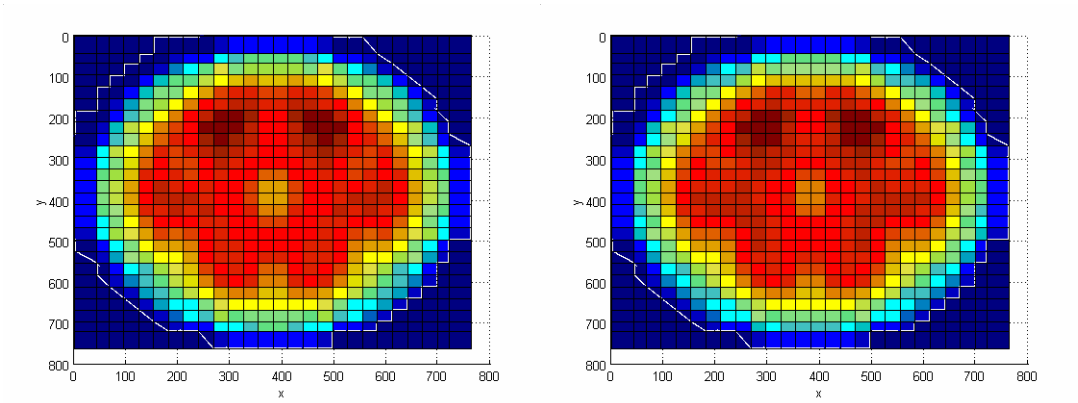

Complete P_1 Original Calculation

Figure 5: Flux shape at plane 4 for both methods (thermal flux, xy surface)

Both methods present a tilt but as Figure 6 shows, the complete P_1 method gives rise to a slightly smaller tilt in the center region and a higher one in the periphery. In the center region, as more neutrons are absorbed, a neutron current from the top of the reactor will be directed downwards to compensate the loss. A stronger coupling coefficient in the fast energy group will tend to correct the tilt. In the P_1 method, the presence of light water has an impact shown through the presence of the down-scattering term of the anisotropic cross-sections. The peripheral tilt is caused by the higher fast scattering coefficient. Since the flux is higher in the top portion of the reactor than at the bottom, the leakage will tend to react accordingly.

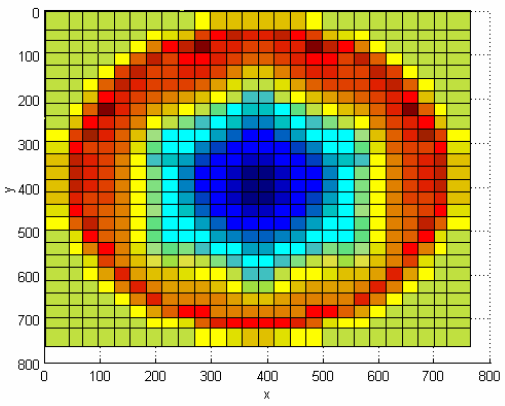

Figure 6: Difference between the two methods at plane 4 (thermal flux)

In order to show the importance of the down-scattering terms in the equation system, a modification was brought to the program. The anisotropic scattering cross-sections were forced to zero, except for the within group terms. In doing so we get a solution that is almost the equal to the original solution with diffusion coefficients. We then compare the complete P_1 method with this new solution, and thereby helping to determine the exact cause of the observed variations.

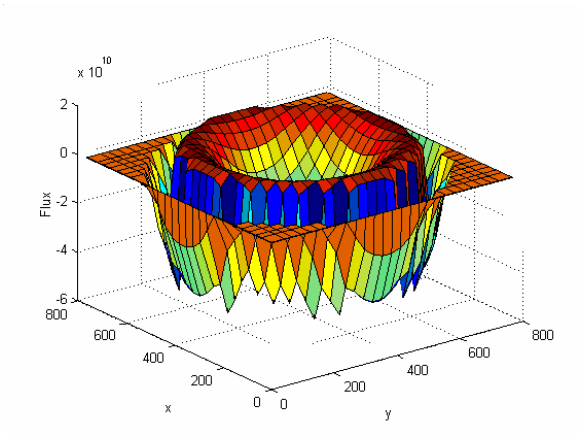

Figure 7 : Energy dependence in a reactor without devices (plane 6, thermal group)

Figure 7 shows the influence of the down-scattering anisotropic cross-section on the flux distribution. First of all, the variations are of the order of 10^{10} while the flux level is in the range of 10^{14}. This shows that the effect is in practice negligible in a reactor without any devices. The flux in the reflector tends to increase if we neglect the down-scattering term.

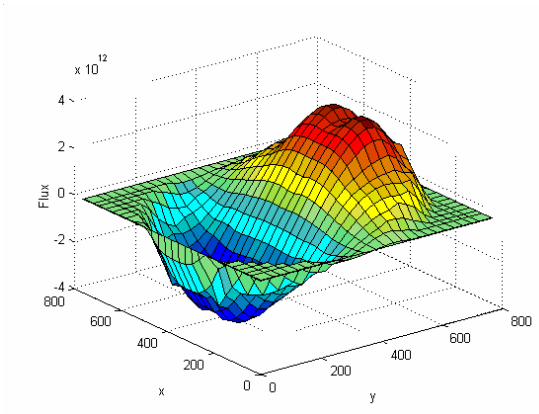

Figure 8 : Energy dependence in a reactor with devices (plane 4, thermal group)

Figure 8 reveals a greater variation than that of Figure 7. The order of the variation is 10^{12}, which will have a noticeable impact on the total flux. We can also observe that the variation shown in figure 7 is completely negligible in the presence of control devices. The complete P_1 method predicts a higher flux at the bottom of the reactor by about 1% and a decrease of the same amount at the top. This means that using the down-scattering term will have a positive effect in correcting the tilt.

4.2 Dynamic Calculations

The first dynamic calculation was performed on a CANDU-6 reactor model with the control devices placed at nominal position. The transient consists of a movement of the central adjuster rod. The rod is maintained at nominal position for first 5 seconds, then it is pulled out of the reactor for thirty seconds, then the movement direction is reversed so that the rod moves back into the core in thirty seconds.

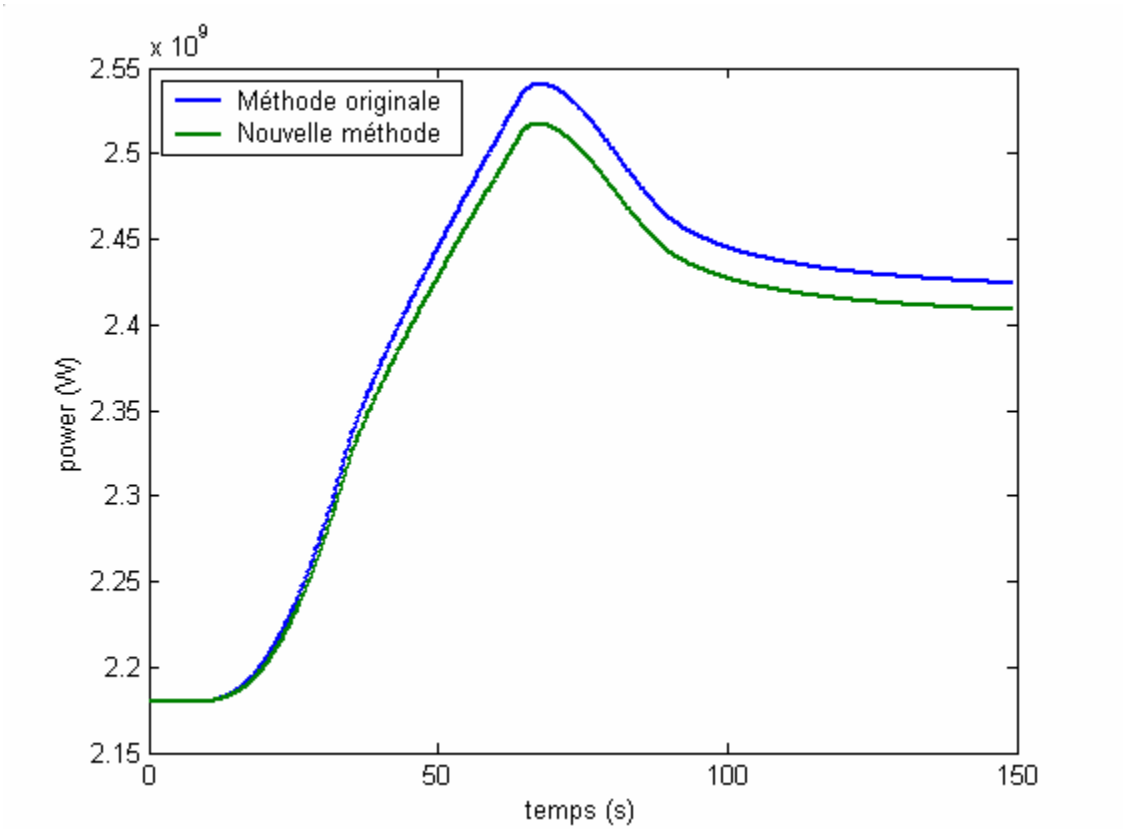

Figure 9 : Reactor power versus time following movement of the center control rod.

From this simulation, we see that both methods show a very similar power transient. As the rod is removed, the new method will tend to predict a higher value than the original method. This variation is due to the flatter flux distribution of the new method. Reducing the center flux will affect the original method more than the complete P_1 method. The flux distribution of this simulation is very close to the distribution found in the static case. The largest positive variations appear in the reflector region with a depression in the center.

The next simulation starts with all devices in their nominal position. After 5 seconds, the central rod is pulled out of the core in thirty seconds. The rod keeps this final position for the rest of the 125 second transient.

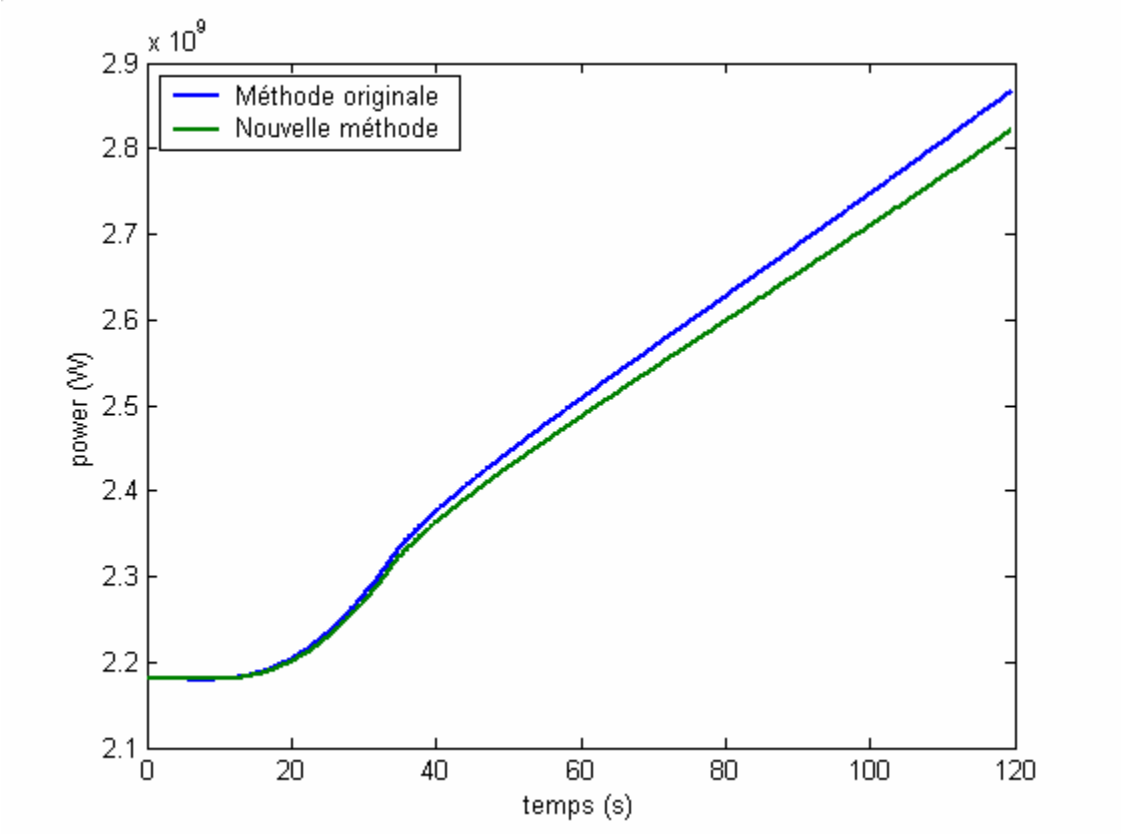

Figure 10 : Reactor power versus time following the removal of the center control rod.

In this case, we see the same separation occurring between the reactor powers given by the two methods. The complete P_1 method (in green) predicts a smaller power increase from the removal of the center rod. Again, this situation can be attributed to the flatter flux distribution of complete P_1 method. By removing the center control rod, the original method, which already predicted a higher center flux, will see the center fluxes increase faster than the complete P_1 method. The difference between the flux distributions shows an increase in the absolute value of the center depression that we are able to see in the static case.

5. Conclusion

The complete P_1 method predicts in every case a higher peripheral flux in a typical CANDU-6 reactor. It was also shown that there is non-negligible anisotropic energy dependence at the interface of the liquid zone controllers due to the presence of light water.

The peripheral thermal flux in the reference reactor sees its value increasing of about 3% while the center thermal flux decreases of about 1%. The complete P_1 has a flattening effect on the flux distribution in the reactor. The variations are mostly caused by the

increase of the coupling coefficient of the fast energy group compared to the original method. Since neutrons are born in the fast energy group, the variation will directly affect the thermal flux distribution.

The down-scattering anisotropic cross-sections of the complete P_1 method reduces the tilt that is caused by the presence of the liquid zone controllers. The nature of these devices creates a tilt but the importance of this tilt is not well represented by the diffusion theory which tends to overestimate it. The complete P_1 method offers a correction to this problem but the actual concordance with experimental results has yet to be determined.

The complete P_1 method should reduce the gap between diffusion theory and transport theory by giving a more realistic prediction of the neutron flux on at material interfaces. However, the full accuracy of the method depends on the rigorous homogenization of the anisotropic cross-sections.

References

1. HENRY, A.F., *Nuclear Reactor Analysis*, The MIT Press, Cambridge, Massachusetts, (1975).
2. ROZON, D., *Introduction à la cinétique des réacteurs nucléaires*, Éditions de l'École Polytechnique de Montréal, Montréal, (1992).
3. ASH, M., *Nuclear Reactor Physics*, McGraw-Hill, New York, (1979).
4. BELL, G., GLASSTONE, S., *Nuclear Reactor Theory*, Robert E.Krieger Publishing Company, Huntington, New York, (1979).
5. LARSEN, E., POMRANING, G.C., *The Pn Theory as an Asymptotic Limit of Transport Theory in Planar Geometry – I:Analysis*, Nuclear Science and Engineering, 109, 49-75, (1991).
6. RULKO, R., LARSEN, E., POMRANING, G.C., *The Pn Theory as an Asymptotic Limit of Transport Theory in Planar Geometry – II: Numerical Results*, Nuclear Science and Engineering, 109, 76-85, (1991).
8. VARIN, E., HÉBERT, A., ROY, R., KOCLAS, J., *A User Guide for DONJON*, IGE-208, École Polytechnique de Montréal, (May 2000).
9. MARLEAU, G., HÉBERT, A., ROY, R., *A User Guide for DRAGON*, IGE-174, École Polytechnique de Montréal, (September 2001).